

Mesons Above The Deconfining Transition

QCD-TARO Collaboration: Ph. de Forcrand¹, M. García Pérez², T. Hashimoto³, S. Hioki⁴, H. Matsufuru^{5,6}, O. Miyamura⁶, A. Nakamura⁷, I.-O. Stamatescu^{5,8}, T. Takaishi⁹ and T. Umeda⁶

¹SCSC, ETH-Zürich, CH-8092 Zürich, Switzerland

²Dept. Física Teórica, Universidad Autónoma de Madrid, E-28049 Madrid, Spain

³Department of Applied Physics, Faculty of Engineering, Fukui University, Fukui 910-8507, Japan

⁴Department of Physics, Tezukayama University, Nara 631-8501, Japan

⁵Institut für Theoretische Physik, Univ. Heidelberg D-69120 Heidelberg, Germany

⁶Department of Physics, Hiroshima University, Higashi-Hiroshima 739-8526, Japan

⁷Res. Inst. for Information Science and Education, Hiroshima University, Higashi-Hiroshima 739-8521, Japan

⁸FEST, Schneilweg 5, D-69118 Heidelberg, Germany

⁹Hiroshima University of Economics, Hiroshima 731-01, Japan

(May 19, 2019)

We analyze mesonic correlators in *temporal* and *spatial* direction below and above T_c in quenched lattice *QCD*. We find different *pole* and *screening* masses, indication for the persistence of mesonic bound states up to $T \sim 1.5T_c$, and signals of plasma formation.

PACS numbers: 12.38.Gc, 12.38.Mh

With increasing temperature we expect the physical picture promoted by *QCD* to change according to a phase transition where chiral symmetry restoration and deconfinement may simultaneously occur (they are both related to symmetries concerning fundamental matter observables). For model independent non-perturbative results concerning the vacuum and hadron properties, one attempts lattice Monte Carlo studies [1].

Since $T > 0$ breaks Lorentz symmetry the Euclidean formulation of the finite temperature theory specifies a “temperature” (Euclidean time, t) axis (see, e.g., [2]). This makes physics appear differently depending on which direction we probe. For instance, the string tension measured from *space - space* Wilson loops does not vanish above T_c , in contrast to the one measured from *space - time* loops. *Therefore we need to investigate hadronic correlators with full “space-time” structure, in particular the propagation in the Euclidean time.* The latter, however, poses special problems because of the inherently limited *physical length* of the lattice, $l_\tau = 1/T$. To preserve a reasonably fine discretization of the time axis (needed in order to follow the details of the time-dependence of the correlators), while avoiding prohibitively large lattices, we use different lattice spacings a_σ, a_τ in space and in time, with $a_\sigma/a_\tau = \xi > 1$. This is realized by using anisotropic couplings, i.e.:

$$S_{\text{YM}} = -(\beta/3)(\gamma_G^{-1} \text{ReTr} \square_{\sigma\sigma} + \gamma_G \text{ReTr} \square_{\sigma\tau}) \quad (1)$$

for the Wilson Yang-Mills action. Then $\xi = \xi(\beta, \gamma_G)$ and the temperature is $T = 1/l_\tau = \xi/N_\tau a_\sigma$. To determine ξ (“calibration”), correlation functions F in different directions are calculated at $T \simeq 0$ and required to show

isotropy in physical distances, i.e. under rescaling of the lattice time distances by ξ :

$$F^\sigma(z) = F^\tau(t = \xi z). \quad (2)$$

In a quenched simulation, after the Yang-Mills calibration, we calculate hadron correlators from the action

$$S_F = 2\kappa_\sigma \bar{\Psi} W \Psi, \quad \kappa_\sigma^{-1} = 2(m_0 + 3 + \gamma_F), \quad (3)$$

$$W = 1 - \kappa_\sigma \left(\sum_i \Gamma_i^+ U_i T_i + \gamma_F \Gamma_4^+ U_4 T_4 + \text{“h.c.”} \right) \quad (4)$$

($\Gamma_\mu^\pm = 1 \pm \gamma_\mu$, $\gamma_\mu^2 = 1$, T_μ lattice translation operators and m_0 the bare quark mass) and tune γ_F to obtain the same ξ when the requirement (2) is applied to these correlators. If the YM and fermionic actions lead to strong artifacts, (2) cannot be fulfilled simultaneously for all observables and the result depends in particular upon the action [3].

We use $\beta = 5.68$, $\gamma_G = 4$ on lattices of $12^3 \times N_\tau$ with $N_\tau = 72, 20, 16$ and 12 . From the peak of the Polyakov loop susceptibility we find T_c at N_τ slightly above 18, which fixes for the above lattices $T \simeq 0, 0.93T_c, 1.15T_c$ and $1.5T_c$ [4]. We present two sets of results:

- *Set-A* represents a prospective study of the temperature dependence of the *pole* masses. The Yang-Mills calibration is done using Wilson loops and we find a ξ ranging between 5.3 for the widest loops in eq. (2) and 6.3 for the narrowest loops. We use an average $\xi = 5.9$ and we find $\gamma_F = 5.4$ and $a_\sigma^{-1} \simeq 0.81$ GeV from the heavy quark potential, which gives $T_c \sim 265$ MeV.

- *Set-B* represents a more precise analysis of the T dependence of *pole* and *screening* masses and other properties of the hadronic correlators for various quark masses. The calibration uses ratios of Wilson loops, which are more adequate for requiring physical isotropy than the Wilson loops themselves [3]. The ambiguity in ξ is reduced, we find $\xi \simeq 5.3(1)$, $a_\sigma^{-1} \simeq 0.85$ GeV and $T_c \sim 250$ MeV.

The calibration of *Set-A* overestimates ξ and, correspondingly, γ_F , leading to a certain distortion of the quark propagators. Both sets, however, appear to give a consistent physical picture. The various parameters are given in the Table. Details will be given in a forthcoming paper [5]. Because we use variational wave-

functions to create near-ground-state mesons, we gauge-fix to Coulomb gauge. We use periodic (anti-periodic) boundary conditions in the spatial (temporal) directions. Note that since a quenched calculation has to be understood as an approximation to a full simulation one has to make sure that the Polyakov loop sector chosen by center-symmetry breaking above T_c is the real one.

Increasing the temperature is expected to induce significant changes in the structure of the hadrons (see, e.g. [6] for reviews). Two “extreme” pictures are frequently used for the intermediate and the high T regimes, respectively: the weakly interacting meson gas, according to which we expect the mesons to become effective resonance modes with a small width and shift in the mass due to the interaction; and the quark-gluon plasma (QGP), where the mesons should eventually be lost. These genuine temperature effects should be reflected in the low energy structure in the mesonic channels. But this structure cannot be observed directly, due to the inherently short physical temporal distance. Our strategy is the following: we fix at zero temperature a mesonic source which gives a large (almost 100%) projection onto the ground state. Then we use this source to determine the changes induced by the temperature on the ground state. From the above considerations this is a reasonable procedure in a picture where the mesons interact weakly with other hadron-like modes, thus if the observed changes are small. The appearance of large changes will signal the breakdown of a weakly interacting gas picture and there we shall try to compare our observations with those given by the QGP picture. In this case we no longer have a good justification to use that source as representative of the meson. Our assumption is that it still projects onto the dominant low energy states in the spectral function.

The correlators investigated are of the form:

$$G_M(x, t) = \sum_{\mathbf{z}, \mathbf{y}_1, \mathbf{y}_2} w_1(\mathbf{y}_1) w_2(\mathbf{y}_2) \langle \text{Tr} \left[S(\mathbf{y}_1, 0; \mathbf{z}, t) \gamma_M \gamma_5 S^\dagger(\mathbf{y}_2, 0; \mathbf{z} + \mathbf{x}, t) \gamma_5 \gamma_M^\dagger \right] \rangle \quad (5)$$

with S the quark propagator and $\gamma_M = \gamma_5, \gamma_1, 1$ and $\gamma_1 \gamma_5$ for $M = Ps$ (pseudoscalar), V (vector), S (scalar) and A (axial-vector), respectively. We use point and smeared (exponential) *quark sources*:

$$w_{1,2}(\mathbf{y}) \sim \delta(\mathbf{y}) \text{ (point), } w_{1,2}(\mathbf{y}) \sim \exp(-ay^p) \text{ (exp.)} \quad (6)$$

We fix the exponential source taking the parameters a, p in (6) from the observed dependence on \mathbf{x} of the temporal Ps correlator measured with *point-point* source at $T \simeq 0$ (see Table). The results of a variational analysis using *point-point*, *point-exponential* and *exponential-exponential* (*exp-exp*) quark sources indicate that the latter ansatz projects practically entirely on the ground state. This is well seen from the effective mass – see Fig. 1 [8]. Therefore we use for our analysis the *exp-exp* sources in the Table. We now present the results. All masses are given in units of a_τ^{-1} , i.e. we plot *mass* $\times a_\tau$.

a) Effective pole masses. In Fig. 2 we show the effective mass $m(t)$ of the Ps and V time-propagators at $T \simeq 0.93T_c, 1.15T_c$ and $1.5T_c$ for *Set-A* and *Set-B* data. Comparing with $T \simeq 0$ (Fig. 1) we notice practically no change at $T \simeq 0.93T_c$, while above T_c clear changes develop: the effective mass depends more strongly on t , it increases significantly, and the Ps and V reverse their positions. The similarity between *Set-A* and *Set-B* indicates that the overestimation of ξ for *Set-A* is unimportant.

Because of the large changes at $1.5T_c$ we compare the situation here with the QGP picture. For this we calculate mesonic correlators using, with the same source, free quark propagators: S_0 instead of S in (5), with $\gamma_F = \xi = 5.9$ for *Set-A* and $\gamma_F = \xi = 5.3$ for *Set-B*. The comparison – see Fig. 2 – is not quantitative, since we do not know exactly what free quark mass we should use (the data shown are taken for $m_0 = m_q a_\sigma = m_q a_\tau \xi = 0.1$), but similarities are apparent. Generally, above T_c $m(t)$ shows stronger t -dependence, which means that the spectral function selected by the *exp-exp* source no longer has just one, narrow contribution, as for $T < T_c$.

b) Wave functions. For the *Set-B* we have also analyzed the behaviour of the temporal meson correlators with the distance between the quark and anti-quark at the sink. In Fig. 3 we compare the Ps wave functions normalized at $x = 0$, $G_{Ps}(x, t)/G_{Ps}(0, t)$, at several t for $T \simeq 0.93T_c$ (which is very similar to $T \simeq 0$) and $T \simeq 1.5T_c$ at our lightest quark mass ($\kappa_\sigma = 0.086$) and for the free quark case ($m_q a_\sigma = 0.1, \gamma_F = \xi = 5.3$). Our *exp-exp* source of *Set-B* appears somewhat too broad at $T \simeq 0.93T_c$: the quarks go nearer each other while propagating in t . Interestingly enough, this is also the case at $T \simeq 1.5T_c$: the spatial distribution starting from this source shrinks and stabilizes indicating that even at this high temperature there is a tendency for quark and anti-quark to stay together. This is in clear contrast to the free quark case which never shows such a behaviour regardless of the source (in Fig. 3 we use the *exp-exp* source). Hence the only effect of the temperature on the wave function is to make it slightly broader. The same holds also for the other mesons at all quark masses.

c) Pole vs screening masses. On the *Set-B* data we fit the Ps , V , S and A time-correlators to single hyperbolic functions in the regions: 27-36 ($T \simeq 0$ [9]), 8-10 ($T \simeq 0.93T_c$), 6-8 ($T \simeq 1.15T_c$) and 4-6 ($T \simeq 1.5T_c$). Above T_c these masses may be attributed to the tentative states described by the wave functions discussed above. Judging from the effective mass plots, Fig. 2B, they may be somewhat overestimated. Since the spatial physical distance is reasonably large we extract the *screening* masses from spatial correlators with *point-point* source in the range $z = 5 - 6$ at all T (a gauge invariant extended source leads to similar results). At $T \simeq 0.93T_c$ the z -correlators are very similar to those at $T \simeq 0$, at $z = 5$ the effective masses do not reach a plateau but no longer depend on the source. Above T_c , the effective masses

seem to reach a plateau beyond $z = 4$. The results for m and $m^{(\sigma)}$ at $\kappa_\sigma = 0.086$ are shown in Fig. 4. In QGP regime at high T one expects $m^{(\sigma)} \sim 2\pi/N_\tau \sim 0.39(0.52)$ in units of a_τ^{-1} for $T \simeq 1.15T_c(1.5T_c)$, respectively.

The *pole* and *screening* masses (mass squared for P_s below T_c [10]) are linearly extrapolated in $1/\kappa = 2m_0 + 8$ to the chiral limit from the 3 quark masses analyzed (the *Set-A* data do not agree with this extrapolation because of the ξ overestimation). This gives at $T \simeq 0$ the critical value $\kappa_c = 0.1714(1)$. Fitting here the experimental ρ mass gives $a_\sigma^{-1} \simeq 1.18$ GeV from both the *pole* and the *screening* mass. The large difference between $a_\sigma^{-1}(\rho)$ and a_σ^{-1} from the heavy quark potential indicates significant discretization effects, hence a translation of these lattice results into physical parameters is only approximative, while statements about ratios and relative changes are more accurate. Up to T_c *screening* and *pole* masses remain similar, while above T_c the former become much larger than the latter, both at finite quark mass and in the chiral limit – see Fig. 4. A similar behaviour is obtained in an NJL effective model [11], increasing π masses are also obtained in [12]. To succinctly quantify this behaviour we introduce a phenomenological parameter:

$$R = \frac{m^{(\sigma)} - m}{m^{(\sigma)} + m} \xrightarrow{QGP} 1 - \frac{2m_q}{\pi T}, \quad m_q \ll T \ll a_\tau^{-1}. \quad (7)$$

Since $R \rightarrow 1$ for $T \gg T_c$ it can serve as indicator for approaching the QGP regime. For results see Fig. 5.

In conclusion, our quenched QCD analysis shows that the changes of meson properties with temperature are small below T_c , while above T_c they become more important and more rapid, but not abrupt. The behaviour of the wave functions suggests that it makes sense to speak of dominant low energy excitations in the meson channels, which we can characterize by a *pole* mass even well above T_c . The variation with t of the effective mass above T_c may indicate the appearance of a resonance width, although it may simply reflect the uncertainty in our treatment of the low energy states. We see chiral symmetry restoration above T_c , with the P_s and V *pole* masses increasing quickly above T_c and the *screening* masses increasing even faster toward the QGP limit at high T . The change in the ordering of the splittings could be accounted for by an admixture of free quark propagation in the mesonic channels at sufficiently large T . The exact amount of splitting among the channels may, however, be affected by the uncertainty of our fermionic calibration.

A possible physical picture is this: The mesons subsist above T_c (up to at least $1.5T_c$) but are becoming unstable and interact with a significant quark-gluon plasma component. Our results are consistent with this picture, but there may be also other possibilities (cf [13], cf [6] and references therein). Notice also that since this is a quenched simulation, the dynamics is incomplete.

A study of the topological properties of the configurations using the *improved cooling* method [14], to be

presented elsewhere, indicates an accompanying change in the vacuum structure across T_c , with a drop of the topological susceptibility and a qualitative modification of the instanton ensemble which above T_c seems to contain more fluctuations at close range [15].

Further work is needed in order to remove the uncertainties still affecting this analysis. This concerns particularly the calibration and the question of an unambiguous definition of the hadron states at high temperature. We shall also try to extract information directly about the spectral function of the hadronic correlators [16].

Acknowledgments: We thank JSPS, DFG and the European Network “Finite Temperature Phase Transitions in Particle Physics” for support. H.M. thanks T. Kunihiro for interesting discussions. The calculations have been done on AP1000 at Fujitsu Parallel Comp. Res. Facilities and Intel Paragon at INSAM, Hiroshima Univ.

- [1] For a recent review see: E. Laermann, Nucl. Phys. B (Proc. Suppl.) **63A-C** (1998) 114.
- [2] N.P. Landsman and Ch.G. van Weert, Phys. Rep. **145** (1987) 141.
- [3] QCD-TARO: M. Fujisaki et al., in *Multi-scale Phenomena and their Simulation*, F. Karsch, B. Monien and H. Satz eds., World Scientific (Singapore 1997) 208.
- [4] QCD-TARO: M. Fujisaki et al., Nucl. Phys. B (Proc. Suppl.) **53** (1997) 426.
- [5] QCD-TARO: Ph. de Forcrand et al., in preparation.
- [6] H. Meyer-Ortmanns, Rev. Mod. Phys. **68** (1996) 473; H. Satz, hep-ph/9706342.
- [7] T. Hashimoto, A. Nakamura and I.-O. Stamatescu, Nucl. Phys. **B400** (1993) 267.
- [8] The effective mass $m(t)$ is obtained by using the ansatz $\text{const} \times \cosh(mt)$ on pairs of points $t, t+1$.
- [9] For S and A we used $t : 12 - 20$ because of larger statistical errors at high t . For the S -meson mass we only use the connected correlator.
- [10] We assume that the pseudoscalar should still extrapolate in mass squared at $T \simeq 0.93T_c$. Above T_c the κ dependence is very weak and the extrapolation is anyway not sensitive to the ansatz. Details will be given in [5].
- [11] T. Hatsuda and T. Kunihiro, Phys. Rep. **247** (1994) 221.
- [12] J. Berges, D.U. Jungnickel and C. Wetterich, hep-ph/9705474, to appear in Phys. Rev. D.
- [13] C. DeTar and J. Kogut, Phys. Rev. **D36** (1987) 2828; C. DeTar, Phys. Rev. **D37** (1988) 2328.
- [14] Ph. de Forcrand, M. García Pérez and I.-O. Stamatescu, Nucl. Phys. **B499** (1997) 409.
- [15] Ph. de Forcrand et al., hep-lat/9810033, proc. Latt98, Nucl. Phys. B (Proc. Suppl.) (to appear).
- [16] QCD-TARO: Ph. de Forcrand et al., Nucl. Phys. B (Proc. Suppl.) **63** (1998) 460.

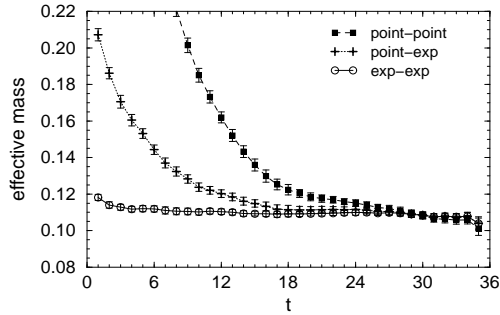


FIG. 1. Effective pseudoscalar *pole* mass $m(t)$ in units of a_τ^{-1} vs t , for various sources at $T \simeq 0$ (*Set-A*).

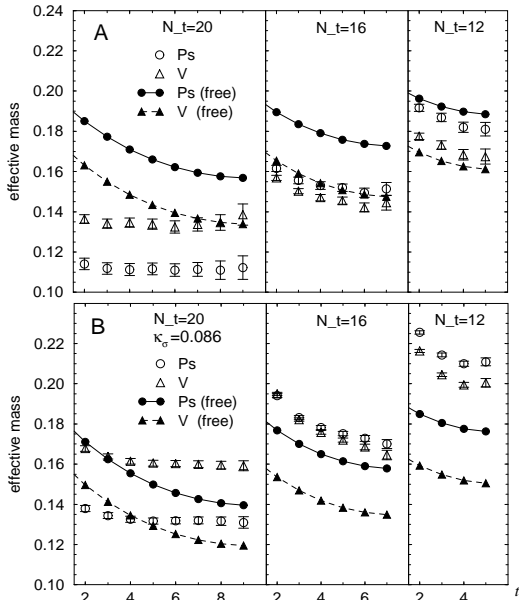


FIG. 2. From left to right, effective mass $m(t)$ in units of a_τ^{-1} at $T \simeq 0.93$, 1.15 and $1.5T_c$ (open symbols) vs t . Also shown are the effective masses from the same correlators calculated using free quarks. A: *Set-A*, B: *Set-B*, $\kappa_\sigma = 0.086$.

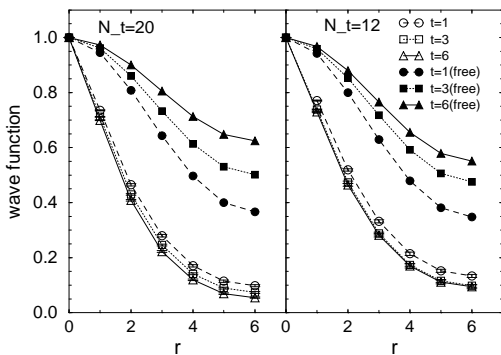


FIG. 3. The Ps wave functions (*Set-B*, $\kappa_\sigma = 0.086$, *exp-exp* source) normalized at $r = 0$ for each t vs quark separations r at $t = 1, 3$ and 6 , using full and free propagators. We show data at $T \simeq 0.93T_c$ and $T \simeq 1.5T_c$.

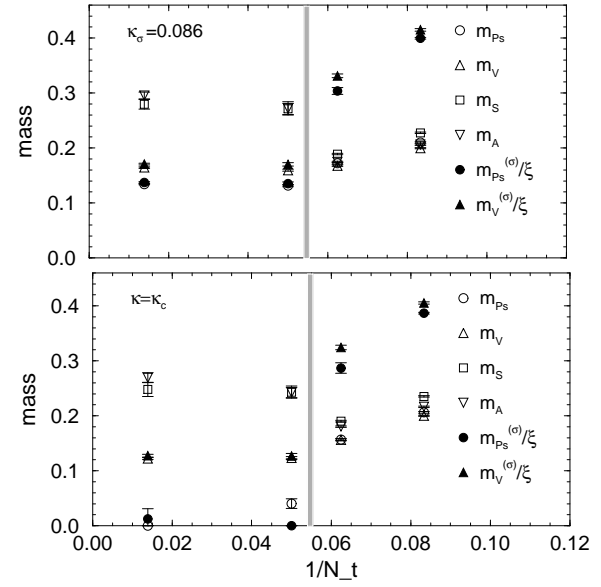


FIG. 4. Temperature dependence of the *pole* mass m (open symbols) and *screening* mass $m^{(\sigma)}$ (full symbols) in units a_τ^{-1} , for *Set-B*, $\kappa_\sigma = 0.086$ (upper plot) and in the chiral limit (lower plot). The vertical gray lines indicate T_c . The data correspond to $T \simeq 0$, $0.93T_c$, $1.15T_c$ and $1.5T_c$.

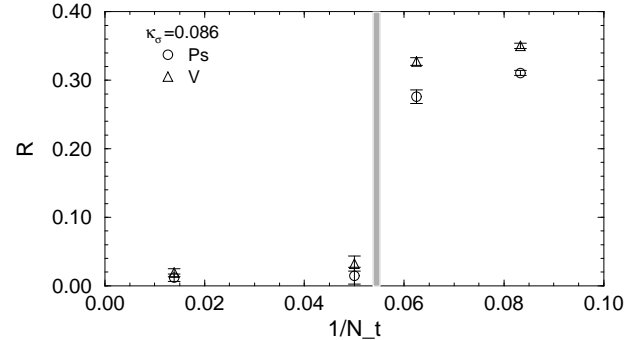


FIG. 5. Temperature dependence of R , eq. (7). The vertical gray line indicates T_c . The data correspond to $T \simeq 0$, $0.93T_c$, $1.15T_c$ and $1.5T_c$.

set	κ_σ	γ_F	m_{Ps}	m_V	a	p
A	0.068	5.4	0.109(1)	0.132(2)	0.442	1.298
B	0.081	4.05	0.178(1)	0.196(1)	0.379	1.289
	0.084	3.89	0.149(1)	0.175(1)	0.380	1.277
	0.086	3.78	0.134(1)	0.164(1)	0.380	1.263

TABLE I. Simulation parameters and meson masses at $T \simeq 0$ (in units a_τ^{-1}). The source parameters a , p eq. (6) are extracted from the $T \simeq 0$ wave function.